Adv. Electron. Mater. **2017**, 1600378, DOI: 10.1002/aelm.201600378

Article type: Progress Report

Electronic Properties of Copper(I) Thiocyanate (CuSCN)

Pichaya Pattanasattayavong, Vinich Promarak and Thomas D. Anthopoulos*

Dr. P. Pattanasattayavong, Prof. V. Promarak
Department of Materials Science and Engineering, School of Molecular Science and Engineering, Vidyasirimedhi Institute of Science and Technology (VISTEC), Rayong, 21210, Thailand
E-mail: pichaya.p@vistec.ac.th

Prof. T. D. Anthopoulos
Department of Physics and Centre for Plastic Electronics, Blackett Laboratory, Imperial College London, London, SW7 2AZ, United Kingdom

Keywords: Copper(I) thiocyanate (CuSCN); wide band gap semiconductor; hole transport; electronic band structure; defects; density functional theory (DFT)

Abstract

With the emerging applications of copper(I) thiocyanate (CuSCN) as a transparent and solution-processable hole-transporting semiconductor in numerous opto/electronic devices, fundamental studies that cast light on the charge transport physics are essential as they provide insights critical for further materials and devices performance advancement. The aim of this article is to provide a comprehensive and up-to-date report of the electronic properties of CuSCN with key emphasis on the structure-property relationship. The article is divided into four parts. In the first section, we review recent works on density functional theory calculations of the electronic band structure of hexagonal β-CuSCN. Following, various defects that may contribute to the conductivity of CuSCN are discussed, and newly predicted phases characterized by layered 2-dimesnional-like structures are highlighted. Finally, a summary of recent studies on the band-tail states and hole transport mechanisms in solution-deposited, polycrystalline CuSCN layers is presented.

1. Introduction

Copper(I) thiocyanate (CuSCN) has been attracting increasing interest for the use as an optically transparent hole-transporting intrinsic semiconductor in various opto/electronic devices including thin-film transistors (TFTs),[1] organic-light emitting diodes (OLEDs),[2] bulk-heterojunction (BHJ) organic solar cells,[3,4] extremely thin absorber (ETA) solar cells,[5] dye-sensitized solar cells (DSSCs),[6] and perovskite solar cells (PSCs).[7] Despite the breadth of the high potential technological applications (see also a review by Wijeyasinghe and Anthopoulos[8] on applications of CuSCN), the study into the electronic properties of CuSCN is still in the early stage. Some key aspects that provide the groundwork have recently been investigated both theoretically and experimentally, and it is the aim of this article to summarize these important works.

One important impediment in the development of inorganic semiconductors for plastic/organic electronics and related applications is the scarcity of suitable hole-transporting, wide band gap semiconductors. The arduous pursuit to predict, synthesize, and apply such materials has focused on metal oxide compounds and yielded only limited success, particularly when compared with the rapid advances of the electron-transporting counterparts such as ZnO, In_2O_3, or indium-gallium-zinc oxide (IGZO). Among the range of studied *p*-type oxides, only Cu_2O, SnO, and NiO have been shown to yield functional opto/electronic devices (see a recent review on *p*-type oxide semiconductors by Wang *et al*.[9]), but their performance is still lacking, especially when high transparency in the visible range is of crucial importance. In addition, their stability and processability are also of concern. On the other hand, CuSCN, a Cu(I) pseudohalide compound, has been shown to be an intrinsic *p*-type inorganic semiconductor with a wide band gap ($\geq$3.5 eV)[10–12] and appropriate electronic levels that allow efficient hole injection/extraction while simultaneously blocking electron transport.[2–4] The latter is a characteristic not shared by Cu_2O, SnO, and NiO primarily due to difficulties associated with controlling their stoichiometry. As a result, CuSCN has successfully been

employed as a universal, highly transparent hole-injecting/extracting/transporting layer in a wide range of applications.[8] Additionally, CuSCN is chemically stable[13–15] and can be easily prepared at high purities as well as processed from solution-phase at low temperatures.[16–19] Moreover, owing to its quasi-molecular nature, CuSCN can be chemically modified;[20] in fact, the properties and applications of CuSCN derivatives are still awaiting exploration and could potentially open up a new range of possibilities.

With an expanding list of important technological applications, it is now essential that the fundamental electronic properties of CuSCN are understood. Herein, we comprehensively review recent works on the electronic and charge transport properties of CuSCN. The band structure and density of states in hexagonal β-CuSCN are first examined to elucidate the underlying basis for the unique combination of excellent hole transporting characteristics and high optical transparency. Defects that could lead to unintentional doping are then considered. Apart from the known bulk α and β phases, recent works on the prediction of layered 2D-like structures of CuSCN are also presented. These newly predicted phases resemble those of the novel 2D metal dichalcogenides and graphene. In addition, models of different surfaces of hexagonal β-CuSCN are also discussed as the orientation of the structure is expected to significantly affect the charge transport. Lastly, studies on the tail of localized states in the mobility gap and the resulting hole transport mechanisms in polycrystalline solution-processed layers of CuSCN are summarized.

2. Electronic Properties of CuSCN

Despite the relatively recent history of CuSCN as a promising hole-transporting material for numerous opto/electronic applications, there have been only a handful of published theoretical studies of the electronic properties of CuSCN, in particular by Jaffe *et al.*,[11] Ji *et al.*,[21] Chen *et al.*,[22] and Tsetseris.[23] These works mainly employ the density functional theory (DFT) calculations for elucidating the electronic structure of the most popular form of CuSCN

(usually observed in experiments), the hexagonal β-CuSCN (**Figure 1**a). The results of valence band (VB) and conduction band (CB) structures of different studies are in line with each other, and the two important characteristics near the band edges are: (1) the strong Cu 3*d* character with some hybridization from the S 3*p* states near the VB edge, and (2) the antibonding π^* character associated with the cyanide portion near the CB edge. These properties lead to the excellent hole transport and the predicted large indirect band gap, both of which result in the dominant *p*-type characteristics and the extremely high transparency in the visible range.

2.1. Electronic Band Structure of CuSCN

Different DFT calculations[11,21,22] have yielded qualitatively consistent results of the band structure of hexagonal β-CuSCN (one set of the results[22] is displayed in Figure 1b whereas the Brillouin zone of a hexagonal lattice[24] is shown in Figure 1c). All of them unanimously predict an indirect band gap with a VB maximum (VBM) at the Γ point and a CB minimum (CBM) at the K point (Figure 1b and 1c). The DFT method employing the generalized gradient approximation (GGA), which is well known to underestimate the band gap, showed a relatively small gap of approximately 2 eV. However, by carrying out the DFT calculation with the Heyd-Scuseria-Ernzerhof (HSE) hybrid functional, Chen *et al*.[22] obtained a value of 3.45 eV which is closer to the experimental values of 3.7-3.9 eV.[11,12,25–27] However, the latter values were mostly obtained via Tauc analysis of the optical absorption spectra assuming a direct band gap (by setting the exponent parameter equal to 2 for the Tauc plot). Pattanasattayavong *et al*.[1] carried out a similar analysis but for both indirect and direct types and obtained values of 3.5 and 3.9 eV, respectively. The lower value of the indirect type seems to corroborate the result from the DFT-HSE method while the higher value may indeed point to the existence of a higher energy transition of a direct type which has also been predicted by Jaffe *et al*.[11] to be at 0.4 eV higher than the lowest transition. On the other hand,

Kim *et al.*,[28] employing the photoelectron spectroscopy (PES) and inverse photoelectron spectroscopy (IPES) to measure the VBM and the CBM of CuSCN, reported a band gap value of 3.65 eV without specifying whether the type was direct or indirect. Also, the values of the band gap described so far are of CuSCN samples with polycrystalline or nanocrystalline morphologies which exhibit a significant and rather extensive absorption tail. Such an absorption feature may be due to the indirect band gap, disorder or non-crystallinity, polymorphism, or a combination of these factors.[11] It should be noted, therefore, that the analysis of the band gap of CuSCN still requires further experimental verification.

Another important characteristic of the band structure of β-CuSCN is the relatively high dispersion near the top of the VB. Generally, for the common wide band gap semiconductors such as In_2O_3, SnO_2, and ZnO, the CBs are highly dispersive while the VBs are flat near the band edges,[29] resulting in *n*-type conductivity and high electron mobility values. On the other hand, calculations have shown that the relative dispersions of the CB and the VB in CuSCN are comparable (see Figure 1b),[11,21,22] suggesting that hole transport is not hindered (and conversely that electron transport is suppressed). The direction of transport is also important due to the alternating planes of Cu and SCN units. Along the *c*-axis of the crystal (along which the Cu and SCN layers alternate), Jaffe *et al.*[11] found that the effective masses (m^* expressed in terms of multiples of the electron rest mass m_0) were similar, i.e., $m^* \approx m_0$ for electrons and $m^* \approx 0.8m_0$ for both heavy and light holes. On the other hand, the electrons and the heavy holes carried effective masses of $m^* \approx 2m_0$ in the *ab* plane whereas the light holes showed a smaller value of $m^* \approx 0.5m_0$. The dispersion characteristics of VB and CB of CuSCN support the dominant hole-transporting properties of this material.

Furthermore, the appropriate level of the VBM (i.e., ionization energy) of CuSCN allows the injection and extraction of holes by common electrodes such as gold or indium tin oxide-based conductors. It is crucial that good Ohmic contacts can be established; otherwise,

the hole-transporting properties may not be useful if the semiconductor's VBM level is too deep or too shallow such that practical carrier injecting electrodes are not available. The reported values of the VBM of CuSCN are typically in the range of -5 to -6 eV as measured by the PES[12,28,30] and electrochemical methods.[31,32] On the other hand, the CBM level of CuSCN determined experimentally via IPES is found to be -2.5 eV.[28] This characteristically shallow CBM energy makes CuSCN an excellent electron-blocking material as already demonstrated in several studies.[2–4,33]

2.2. Density of States in CuSCN

Figure 2a shows the total density of states (DOS) and partial density of states (PDOS) of hexagonal β-CuSCN in more detail. The top of the VB from the VB edge (set at E = 0 eV) to approximately -2.5 eV is strongly dominated by the Cu 3*d* states with some contribution from the S 3*p* states. From -3.5 to -10 eV, there are four sub-bands altogether. The first three sub-bands, centered around -4, -6, and -7 eV, mainly arise from the *p* states of S, C, and N, which may be associated with the π bonding within the –SCN unit. The highest of these three sub-bands (centered around -4 eV) also has contribution from the Cu 3*d* in addition to the S 3*p* and N 2*p* states, possibly suggesting the character of the bonding between Cu and the coordinating S and N as well. The last of the four sub-bands, located around -9 eV, is dominated by the S 3*p* and C 2*p* states, which implies the S–C bond. The photoemission spectrum of CuSCN near the VBM in this energy range is in qualitative agreement with the calculated DOS as displayed in Figure 2b. There are two additional sub-bands deeper in the VB, which predominantly contain the *s* states of S, C, and N. The sub-band around -16 eV is possibly associated with the S–C bond while the sub-band centered at -19 eV may arise from the σ bonding of the cyanide portion. With the increasing binding energy, the VB character of hexagonal β-CuSCN is consisted of: bonding between Cu 3*d* states with some hybridization from S 3*p* states, coordination between Cu 3*d* states and S 3*p* and N 2*p* states, and π bonding

and σ bonding in the –SCN unit, respectively. The dominating Cu 3*d* states near the top of VB allows the hole transport in CuSCN, similar to the case of Cu_2O, also a Cu(I) compound that shows a strong character of Cu 3*d* states at the VBM.[34,35] This is in contrast to the dominant O 2*p* character in the VBM vicinity of important oxide semiconductors such as ZnO, SnO_2, and In_2O_3.[29]

Interestingly, the CB edge, which is dominated by the C 2*p* and N 2*p* states, shows a unique character of the π^* antibonding orbitals of the cyanide part that has no analog in traditional semiconductors. The antibonding characteristics of the CB also results in a CBM located away from the Γ point in the Brillouin zone,[11] leading to the indirect type of the lowest interband transition. The indirect band gap also enhances the optical transparency in the visible range of CuSCN since strong absorption only takes place when the photon energies reach the direct gap which is at a higher energy.

3. Defects in CuSCN

In an early study, Tennakone *et al*.[10] showed that the conductivity of CuSCN could be tuned to be either *p*-type or *n*-type by adjusting the Cu:SCN ratio. Specifically, the authors employed the chemical bath and electrodeposition methods to obtain both types of CuSCN. Based on their chemical methods and analyses, *p*-type CuSCN had a Cu:SCN ratio from 0.92 to 0.96 where *n*-type CuSCN showed a ratio between 1.31 and 1.44. Following, it was also demonstrated that doping CuSCN with SCN could increase its *p*-type conductivity.[36] Therefore, extrinsic *p*-doping of CuSCN has generally been associated with the excess SCN or deficient Cu conditions, and naturally the native defect Cu vacancy (V_{Cu}) is proposed to be the major source of excess holes often observed in CuSCN.[11,21,23] In extrinsically *p*-doped CuSCN, the Fermi level (E_F) has been reported to shift toward the VBM (e.g., 0.63 eV above VBM by Pattanasattayavong *et al*.[12] and 0.75 eV above VBM by Kim *et al*.[28]. Reports on *n*-type conductivity of CuSCN, on the other hand, is not common and, even if attainable, may

not be suitable for practical applications because the CBM is shallow (around -2 to -3 eV with respect to the vacuum level) and would require the use of electrodes with extremely low work function and/or the use of doped injection layers. Next, we discuss relevant types of defects that can influence the conductivity of CuSCN.

3.1. Copper Vacancy

Computational results have shown that Cu vacancies should be stable and result in a shallow acceptor level that can contribute to high hole concentrations in hexagonal β-CuSCN.[11,21,23] The removal of a Cu atom from the lattice causes the neighboring atoms to move only slightly.[11,23] For example, Tsetseris[23] calculated that the distance between S atoms would change from 3.85 Å to 3.71 Å. Jaffe *et al.*[11] reported that the formation energy of a Cu vacancy was around 0.2 eV for a 32-site supercell and estimated that a hole concentration as high as 10^{19} cm^{-3} could be feasible. Interestingly, their calculation result of a larger 72-site supercell (which corresponds to a lower concentration of V_{Cu}) yielded a higher formation energy of 0.55 eV, possibly further suggesting that high concentrations of V_{Cu} are easily obtainable. Results from Ji *et al.*[21] also indicated a similar trend, i.e., a lower V_{Cu} formation energy at a higher concentration; however, their calculated formation energies were rather high (4.45 eV for a 32-site supercell and 5.12 eV for a 72-site supercell). The same authors also reported the effect of a Cu vacancy on the band gap of CuSCN although the results were not straightforward. Specifically, in the case of the 72-site supercell the energy band gap was found to slightly increase while transforming to direct. On the other hand, in the 32-site supercell the band gap remained indirect but increased significantly. The widening of the bandgap in both cases was caused by a corresponding shift in the CB energy.[21]

An acceptor level at about 0.1 eV above the VBM has been reported by Jaffe *et al.*[11] and Ji *et al.*[21] for the Cu vacancy. The latter study also described another acceptor level at 0.02 eV although they did not specify/elaborate on its possible origin.[21] In contrast,

Tsetseris[23] showed that V_{Cu} did not yield an acceptor level but instead caused E_F to move into the VB, leading to strongly enhanced *p*-type conductivity. However, despite the speculation of V_{Cu} being the main contributor of excess holes in CuSCN, its existence and its defect energy level in CuSCN are still awaiting experimental substantiation. To this end, Perera *et al.*[36] reported that doping CuSCN with SCN resulted in an acceptor level at 1 eV above VBM as experimentally observed from a photoluminescence (PL) emission at 460 nm, yet such a deep level should not contribute to a significant increase in conductivity. Interestingly, significant PL emission at ~460 nm in CuSCN has been reported previously and was attributed to surface states originating from $Cu(SCN)_2$ impurities.[37] It is therefore absolutely clear that further work would be required in order to elucidate the origin of these defects.

3.2. Other Native Defects

Another basic vacancy is the removal of the SCN unit (V_{SCN}), which is predicted to yield a donor level and essentially acting as *n*-dopant. Tsetseris[23] reported that V_{SCN} in β-CuSCN lattice would lead to significant changes in the positions of the surrounding atoms, e.g., the Cu-Cu distance would increase from 3.85 Å to 4.33 Å. Jaffe *et al.*[11] also showed that the formation energy of V_{SCN} would be high (i.e., 3.17 eV for a 32-site supercell) even under favorable Cu-rich conditions and still as high as 2.05 eV under degenerate *p*-type conditions (when E_F moves into VB) which would highly favor the creation of compensating donors. These values are much higher than those predicted by the authors for V_{Cu} (0.2 to 0.55 eV) as discussed earlier. Jaffe *et al.*[11] further speculated that V_{SCN} should not exist in significant amount under equilibrium conditions although they may be present in samples which are out of thermodynamic equilibrium, such as those prepared by electrodeposition under certain conditions.[10]

Tsetseris[23] also considered two other isomers of the SCN unit as substitutional defects on SCN site, i.e., NCS and CNS [which can be represented as $(NCS)_{SCN}$ and $(CNS)_{SCN}$]. The formation energies were calculated to be 0.85 eV and 1.58 eV, respectively, implying that they could still exist in small numbers in β-CuSCN. However, the author only stated the rearrangement of the atoms in the thiocyanate group but did not discuss the details regarding the bonding schemes in these isomers. For example, the NCS may exist as a isothiocyanate (N=C=S) in such circumstance and could lead to extra strain from the different bond angles and distances. Isomerism in CuSCN is not uncommon,[38] and these substitutional defects may be an interesting subject of further study.

On the other hand, Jaffe *et al.*[11] examined the possibilities of the SCN unit having some parts missing. In particular, removing the cyanide part (a CN vacancy, V_{CN}, or equivalently a substitutional S on SCN site, S_{SCN}) could serve as another acceptor as the divalent sulfide can accept another electron from the lattice. Indeed, its defect energy level was calculated to be sufficiently shallow for *p*-type doping although its formation energy was not reported. In contrast, removing the sulfide [an S vacancy, V_S, or equivalently a substitutional CN on SCN site, $(CN)_{SCN}$] would likely lead to an inactive neutral defect due to the same charge on the cyanide and thiocyanate ions. The authors also stated that vacancies of only C or N would unlikely exist due to the strong triple bond and speculated that interstitial and antisite defects would not be likely due to the close-packed hexagonal structure of β-CuSCN and the large asymmetry between the Cu and SCN units.

Although a small number of studies as presented above have considered defects in CuSCN, there is still an apparent lack of intensive and extensive investigation into the topic akin to defect studies in other oxide semiconductors.[39–41] A comprehensive study on the formation energies of various defects in different charge states and under different preparation conditions (Cu-rich or Cu-deficient) as a function of E_F would provide a more complete picture of the defect physics and charge compensation in CuSCN.

3.3. Hydrogen Impurities

Tsetseris[23] studied the inclusion of hydrogen impurities in the lattice of hexagonal β-CuSCN. The calculation results of a single hydrogen atom showed that the most stable configurations were the formation of S–H or C–H bonds (**Figure 3**a and 3b) with the corresponding formation energies of 0.6 eV and 0.7 eV, respectively. More importantly, two H impurities that resulted in the hydrogenation of the cyanide [H–CN–H defect as depicted in Figure 3c or equivalently substitutional hydrogenated SCN $(SCNH_2)_{SCN}$] were shown to be significantly more stable as the formation was highly exothermic, lowering the energy by approximately 1 eV with respect to the pristine β-CuSCN lattice and a H_2 molecule in vacuum. The author proposed that the H_2 impurities in the form of hydrogenated cyanide defect could likely exist in real β-CuSCN samples. Another report by Pattanasattayavong *et al.*[12] also showed that some C and N in their CuSCN samples may exist in C=N state instead of the cyanide C≡N state. One of the causes for such observation may be hydrogenation, which would corroborate Tsetseris's findings. However, no final conclusion should be drawn yet until further experiments can confirm the finding. Also, isomerism of the thiocyanate ion may be another explanation for the C=N state.[38]

Regarding the type of defect, the single H impurities (both S–H and C–H) were found to be of acceptor type, and their effects on the electronic structure of β-CuSCN were similar to those of V_{Cu}, i.e., increasing *p*-type conductivity.[23] Contrastingly, the H–CN–H defect was reported to create a state at 0.2 eV below the CBM that could act as a donor level and may lead to the compensation of acceptors.[23] Again, these computational results still require experimental validation.

4. Polymorphs and Surfaces of CuSCN

Most of the results reported to date, both computational and experimental, were associated with the hexagonal β-CuSCN.[18] Another form, α-CuSCN (**Figure 4**a), has also been reported and its structure characterized[16] although it is less observed in experiments. It should also be noted that the β phase also exhibits polytypism, which results from different stacking sequences along the *c*-axis of the lattice. The most studied polytype is the hexagonal 2H corresponding to AB type layer stacking[18] whereas the rhombohedral 3R with the ABC stacking also exists.[17] Tsetseris[23] calculated the energies and electronic properties of these two polytypes of β-CuSCN as well as 4H (ABAC-stacked) and 6H (ABCACB-stacked) and found that they could all co-exist and would exhibit similar properties.

4.1. Predicted Layered Structures of CuSCN

Remarkably, in another paper Tsetseris also theoretically predicted layered 2D-like structures of CuSCN, namely the γ, δ, and ε phases (Figure 4c, 4d, and 4e).[42] Interestingly, the structure of γ-CuSCN was an analog of that of the 2D metal dichalcogenide while δ-CuSCN resembled the graphene honeycomb structure. These two structures are well known for the 2D materials which currently receive tremendous amount of attention. In fact, a structure similar to that of δ-CuSCN has already been reported for β-CuN_3,[43] which is also a pseudohalide compound of Cu(I). The ε phase of CuSCN was also honeycomb-like but with high degree of corrugation. Among the different phases of CuSCN, Tsetseris[42] calculated that the β form was the most stable, followed by the α phase. The layered γ-CuSCN was, however, only slightly higher in energy than α-CuSCN and may possibly be synthesized under the right conditions. The other two phases, δ and ε forms, were significantly higher in energy and thus less stable. The calculated total density of states (DOS) of γ-CuSCN showed that the band gap was widened compared to that of β-CuSCN.[42] Qualitatively, their plot also suggested that the VB of γ-CuSCN became less dispersive while the CB was more dispersive, which may suggest that the hole transport would be impeded in the layered structure.

Building on the previous study on hydrogen impurities in β-CuSCN, Tsetseris also found that adding hydrogen could significantly improve the stability of the layered forms of CuSCN.[44] In fact, the hydrogenation reactions (specifically adding a hydrogen molecule to the cyanide portion) of α-, β-, γ-, and δ-CuSCN were all exothermic. Surprisingly, the fully hydrogenated form of γ-CuSCN (denoted as γ-$CuSCNH_2$) was the second most stable after β-$CuSCNH_2$. However, the band gap of γ-$CuSCNH_2$ was significantly reduced, and the DOS also exhibited the adverse trend on the hole transport similar to the case of γ-CuSCN (less dispersive VB and more dispersive CB).

4.2. Surfaces of CuSCN

The orientation of the CuSCN crystal is also of high importance as it could have implications on the charge transport properties due to the highly anisotropic nature of its structure. One example is the difference in the calculated effective masses in the *ab* plane and along the *c*-axis of the hexagonal β-CuSCN as discussed previously. Electrodeposition-based methods have been shown to be able to tune the orientation between the (001)-terminated and (101)-terminated surfaces [(001) or (101) planes parallel to the substrate surface, respectively, (**Figure 5**)].[45,46] Although for solution-grown CuSCN films the evidence is not yet clear due to the often small layer thicknesses, results also indicate the presence of (101) or (001) surface-oriented crystals.[11,33] Computational results suggested that the (101)- and (001)-orientations of hexagonal β-CuSCN could be stable especially when terminated with Cu, but the most stable surfaces were (100) and (110).[22] This is mainly because the former pair are characterized by polar surfaces exhibiting a permanent dipole, while the latter are non-polar surfaces.

Interestingly, the results from Chen *et al.*[22] showed that the polar surfaces experienced only slight changes in the displacement of the surface atoms and that their partitioned charges were only marginally different from atoms in the bulk, hence supporting

the idea of the existence of polar surfaces. Worth noting, however, is the fact that calculations of the electronic properties of polar and non-polar surfaces (modelled as slabs in the computations) of β-CuSCN yielded different results.[22,23] The DOS of the non-polar (110) and (100) surfaces (Figure 5a and 5b) were similar to that of the bulk. On the other hand, those of the polar (101) and (001) surfaces (Figure 5c and 5d) showed a significant number of states within the band gap. Chen *et al.*[22] proposed that the polar surfaces could be semi-metallic due to the high density of the Cu 4*s* states near E_F, which could in turn be a result of under-coordination of Cu atoms at the surface.

5. Hole Transport Properties of CuSCN

As already discussed earlier, CuSCN has been employed as a hole-transporting layer in numerous opto/electronic devices (see the review on the applications of CuSCN by Wijeyasinghe and Anthopoulos[8]); however, the studies on the hole transport properties of CuSCN are very limited. Pattanasattayavong *et al.*,[1] employing field-effect measurements, obtained hole mobilities between 0.01 and 0.1 $cm^2\ V^{-1}\ s^{-1}$ from solution-processed thin film CuSCN layers. These mobility values further corroborated the hole diffusion coefficients (which are related to hole mobilities via the Einstein relation $D = \mu kT/q$, where D is the diffusion coefficient, μ is the mobility, k is the Boltzmann constant, T is the temperature, and q is the elementary electric charge) which were reported earlier for CuSCN by Mora-Seró *et al.*[47] to be in the range of 0.001 to 0.01 $cm^2\ s^{-1}$ based on impedance spectroscopy measurements. More recently, Pattanasattayavong *et al.*[48] investigated the band-tail states and hole transport processes in CuSCN based on the analyses of field-effect transistors. In addition, Kim *et al.*[28] used the PES technique with He II source to examine the band-tail states of CuSCN and their effects on the charge extraction in organic photovoltaic devices. It should be noted that the CuSCN samples in both studies were thin films cast from sulfide-based solutions at room temperature followed by thermal annealing in nitrogen environment.

5.1. Band Tail States in CuSCN

It is well established that charge carrier transport in semiconductors and their devices is strongly influenced by the densities of states near the band edges. In highly crystalline materials (e.g. single crystals), the VB and CB are sharp, and the transport proceeds via band transport mode (extended states – wavefunctions are highly delocalized). In non-crystalline and polycrystalline materials, however, structural disorder as well as chemical impurities and the presence of grain boundaries between crystalline regions/domains (crystallites) create localized states above the VBM or below the CBM within the band gap, disrupting the band transport. In the case where the DOS of these localized states are distributed near the band edges (within the bandgap) and are manifested as an optical absorption tail often called band-tail states. Since these DOS can exist in the supposedly forbidden gap (hence no longer a true energy gap), the notation "mobility gap" is sometimes used to distinguish the region between the VB and CB edges. The gap in this case refers to the separation between the extended states where band transport takes place and the localized states.

Pattanasattayavong *et al*.[48] employed a method developed by Grünewald *et al*.[49] to analyze the current-voltage characteristics of nanocrystalline CuSCN layer-based field-effect transistors in order to study the band-tail states. Their results showed that the DOS of the tail states followed an exponential distribution with a characteristic energy of around 42 meV (**Figure 6**a), a value which is similar to those of *p*-type amorphous inorganic semiconductors such as a-Si or a-As_2Se_3.[50–52] It was also shown that the dynamic disorder could play an important role as the DOS became narrower with the decreasing temperature although further investigation is required.

Kim *et al*.[28] studied the VB of CuSCN using the PES technique equipped with a He II (40.82 eV) UV source for resolving states near the band edge. The PES spectrum in close proximity of the VBM revealed the existence of exponential tail states extending into the gap

(Figure 6b and inset) with a characteristic energy of around 150 meV (calculated from the digitized image). The latter value is significantly larger than that reported by Pattanasattayavong *et al.*, but the results are in qualitative agreement. To this end, it should be noted that the spectra from PES measurements may be broadened by various effects and may add to the characteristic energy of the tail states distribution. The authors also showed that, when CuSCN was used as a hole-transporting interlayer, the band-tail states could assist with the hole transport between the electrode and the active semiconductor layer by providing the transport pathway. Specifically, the hole injection/extraction barrier is effectively reduced by the presence of the band-tail states even when CuSCN is not heavily doped (E_F still lies at a considerable distance from the VBM). Additionally, Aldakov *et al.*[53] also analyzed the optical absorption tail (Urbach tail) of their electrodeposited CuSCN samples and reported relatively high values of the characteristic energy in the range of 200-240 meV. The authors cited the possible origins as states within the band gap that may originate from internal strain, composition variations, or surface defects.

5.2. Hole Transport in CuSCN

Despite the widespread use of CuSCN as a hole-transporting layer in various optoelectronic devices, the charge carrier transport mechanisms in CuSCN have only been studied recently by Pattanasattayavong *et al.*[48] By investigating the temperature dependence of the field-effect hole mobility of CuSCN-based thin-film transistors, three different transport regimes were identified for solution-processed CuSCN layers. At high temperatures (228-303 K), the transport was strongly thermally activated, a signature of the multiple trapping and release (MTR) mode which is an archetype model for transport in non-crystalline inorganic semiconductors.[54–56] In this case, carriers can still travel as waves (band transport) in the extended states outside the mobility gap but become momentarily trapped by the localized states in the band tail before being released via thermal activation. At intermediate

temperatures (123-228 K), the transport mechanism was also thermally activated but with a smaller energy barrier. Based on similar observations in non-crystalline inorganic semiconductors, the authors proposed that the transport process followed the variable range hopping (VRH) mechanism in this temperature range.[50,55] The thermal activation persists in this regime due to the hopping process in the tail of localized states.

The transition from MTR to VRH could be understood from the temperature dependence of the transport energy, a representative energy level that the carrier transport takes place.[57,58] For MTR mode, this energy coincides with the band edge, i.e., holes are activated from localized states to the extended states in the VB. When temperature decreases, the transport energy moves away from the VB into the tail states, and the transport mode changes to VRH. Further decrease in temperature causes the transport energy to move deeper into the mobility gap toward the E_F. At low temperatures (78-123 K), the data was not conclusive, but the authors speculated that the transport mode in this regime may be the field-assisted hopping. In light of these results it can be concluded that hole transport in solution-processed polycrystalline layers of CuSCN appears to follow similar mechanisms already observed in conventional non-crystalline inorganic semiconductors. Although established theories provide an appropriate starting point for the development of a deeper understanding of charge carrier transport in CuSCN, more work is certainly required. Elucidating the fundamental nature of charge transport in CuSCN and the role of the layer microstructure, in particular, will most definitely lead to improved deposition routes as well as assist towards the design of new materials and devices with improved operating characteristics for a wide range of future opto/electronic applications.

6. Related Materials

To the best of our knowledge, CuSCN is so far the only material in the pseudohalide group of compounds that exhibits semiconducting properties suitable for practical electronic

applications. Another closely related compound, copper(I) selenocyanate (CuSeCN), has also been studied computationally by Tsetseris[42,44] and shown to possibly possess electronic properties akin to those of CuSCN. Based on similar DFT calculations with the sulfur atom replaced by a selenium atom, the natural phase of CuSeCN was also predicted to be the β phase while the α and the 2D-like layered γ phases were less stable,[42] analogous to the case of CuSCN. Although the author did not explicitly study the charge carrier transport properties, the plot of the total DOS of β-CuSeCN could imply that holes may be the dominant charge carriers due to the higher dispersion near VBM than CBM. Another prediction was a smaller band gap for CuSeCN compared to that of CuSCN.[44] CuSeCN has been observed in electrochemical systems,[59,60] but more research is required to understand its properties and uses. Also mentioned in Ref.[42] is copper azide CuN_3 which is isoelectronic to CuSCN and exhibits a layered phase similar to those predicted for CuSCN and CuSeCN.[43,61] However, azides are highly explosive and thus unlikely to be suitable for electronic applications.[62]

It is also noteworthy to acknowledge copper iodide (CuI) as it is a well-known p-type metal halide also based on Cu(I) and has been employed in several device applications as a hole-transporting layer.[63–66] Although the conductivity of γ-CuI is electronic, α-CuI and β-CuI also show strong ionic conductivity[67] and may present a challenge in the development of electronic devices. However, a full discussion on CuI is beyond the scope of this work as it is a common metal halide and does not possess the quasi-molecular nature as in the case of pseudohalides. To this end, Grundmann *et al.*[67] have recently published a comprehensive review of the properties and applications of CuI.

7. Conclusion

We have reviewed key aspects of the electronic and charge transport properties of the quasi-molecular, wide band gap semiconductor CuSCN. Its excellent hole-transporting properties and the high optical transparency can be understood based on the band structure of this rather

unique material. Recent DFT calculations of hexagonal β-CuSCN show that the VBM is mainly composed of Cu 3*d* states with some hybridization from S 3*p* states whereas the CBM is predominantly the antibonding π^* states of the cyanide portion, resulting in a more dispersive VB as compared with conventional wide band gap inorganic semiconductors.[11,22,23] The antibonding character also leads to an indirect band gap which, coupled with the large band gap of ≥3.5 eV, enhances the optical transparency in the visible range. Calculations of various defects in CuSCN also support the predominant *p*-type conductivity observed in various CuSCN samples prepared from different methods. The Cu vacancy is the main candidate for the acceptor-type doping as its formation energy is predicted to be sufficiently low and its defect energy level close to the VB.[11,21,23] Other potential candidates include the CN vacancy and H impurities.[11,23]

Polymorphism in CuSCN has also been studied theoretically.[23] The β-CuSCN is shown to be the most stable phase, followed by the already observed α phase. Three new layered structures have been predicted, namely the γ, δ, and ε phases. The stability of γ-CuSCN is reported to be close to that of the α phase, suggesting the possibility of synthesizing this form. Its structure also resembles that of the 2D metal dichalcogenides, which represent an important class of emerging electronic materials. Different orientations of CuSCN could also have an impact on the carrier transport due to its anisotropic structure (and the high asymmetry between the Cu and SCN units). Polar and non-polar surfaces of hexagonal β-CuSCN are shown to have different DOS.[22,23]

The band-tail states in non-crystalline solution-processed samples of CuSCN have also been studied. The distribution of these localized states is reported to be in an exponential form extending from the VBM into the gap.[28,48,53] Hole transport in this type of CuSCN has been explained based on the theories of multiple trapping and release and variable range hopping.[48] Theoretical models initially developed for conventional non-crystalline inorganic

semiconductors have been shown to offer basic explanation of tail states and hole transport mechanisms in non-crystalline CuSCN.

On the basis of the published literature to date it can be argued that although the general background of semiconductor physics of CuSCN has been laid out, a significant gap in the detailed understanding of the electronic phenomena that govern charge transport in CuSCN still exists. Experimental verifications are also required for many of the properties that have been predicted by theory. As CuSCN becomes more technologically relevant for application as an optically transparent hole-transporting semiconductor in various opto/electronic devices, further studies of its properties are expected to be highly fruitful and critically important.

Acknowledgements

P.P. would like to acknowledge Thailand Research Fund (TRF) for their financial support under the project MRG5980214.

Received: ((will be filled in by the editorial staff))
Revised: ((will be filled in by the editorial staff))
Published online: ((will be filled in by the editorial staff))

References

[1] P. Pattanasattayavong, N. Yaacobi-Gross, K. Zhao, G. O. Ngonggang Ndjawa, J. Li, F. Yan, B. C. O'Regan, A. Amassian, T. D. Anthopoulos, *Adv. Mater.* **2013**, *25*, 1504.

[2] A. Perumal, H. Faber, N. Yaacobi-Gross, P. Pattanasattayavong, C. Burgess, S. Jha, M. A. McLachlan, P. N. Stavrinou, T. D. Anthopoulos, D. D. C. Bradley, *Adv. Mater.* **2015**, *27*, 93.

[3] N. Yaacobi-Gross, N. D. Treat, P. Pattanasattayavong, H. Faber, A. K. Perumal, N. Stingelin, D. D. C. Bradley, P. N. Stavrinou, M. Heeney, T. D. Anthopoulos, *Adv. Energy Mater.* **2015**, *5*, 1401529.

[4] N. D. Treat, N. Yaacobi-Gross, H. Faber, A. K. Perumal, D. D. C. Bradley, N. Stingelin, T. D. Anthopoulos, *Appl. Phys. Lett.* **2015**, *107*, 13301.

[5] Y. Itzhaik, O. Niitsoo, M. Page, G. Hodes, *J. Phys. Chem. C* **2009**, *113*, 4254.

[6] B. O'Regan, D. T. Schwartz, S. M. Zakeeruddin, M. Grätzel, *Adv. Mater.* **2000**, *12*, 1263.

[7] P. Qin, S. Tanaka, S. Ito, N. Tetreault, K. Manabe, H. Nishino, M. K. Nazeeruddin, M. Grätzel, *Nat. Commun.* **2014**, *5*, 1.

[8] N. Wijeyasinghe, T. D. Anthopoulos, *Semicond. Sci. Technol.* **2015**, *30*, 104002.

[9] Z. Wang, P. K. Nayak, J. A. Caraveo-Frescas, H. N. Alshareef, *Adv. Mater.* **2016**, *28*, 3831.

[10] K. Tennakone, A. H. Jayatissa, C. A. N. Fernando, S. Wickramanayake, S. Punchihewa, L. K. Weerasena, W. D. R. Premasiri, *Phys. Status Solidi* **1987**, *103*, 491.

[11] J. E. Jaffe, T. C. Kaspar, T. C. Droubay, T. Varga, M. E. Bowden, G. J. Exarhos, *J. Phys. Chem. C* **2010**, *114*, 9111.

[12] P. Pattanasattayavong, G. O. Ngongang Ndjawa, K. Zhao, K. W. Chou, N. Yaacobi-Gross, B. C. O'Regan, A. Amassian, T. D. Anthopoulos, *Chem. Commun.* **2013**, *49*, 4154.

[13] B. Ptaszyński, E. Skiba, J. Krystek, *Thermochim. Acta* **1998**, *319*, 75.

[14] K. Tennakone, G. S. Shantha Pushpa, S. Punchihewa, G. Epa, *Electrochim. Acta* **1986**, *31*, 315.

[15] Y. Guo, X. Yu, J. Chen, *Corros. Sci.* **2009**, *51*, 1573.

[16] M. Kabešová, M. Dunaj-jurčo, M. Serator, J. Gažo, J. Garaj, *Inorganica Chim. Acta* **1976**, *17*, 161.

[17] D. L. Smith, V. I. Saunders, *Acta Crystallogr. Sect. B Struct. Crystallogr. Cryst. Chem.* **1981**, *37*, 1807.

[18] D. L. Smith, V. I. Saunders, *Acta Crystallogr. Sect. B Struct. Crystallogr. Cryst. Chem.*

1982, *38*, 907.

[19] G. R. R. A. Kumara, A. Konno, G. K. R. Senadeera, P. V. V. Jayaweera, D. B. R. A. De Silva, K. Tennakone, *Sol. Energy Mater. Sol. Cells* **2001**, *69*, 195.

[20] K. M. Miller, S. M. McCullough, E. a. Lepekhina, I. J. Thibau, R. D. Pike, X. Li, J. P. Killarney, H. H. Patterson, *Inorg. Chem.* **2011**, *50*, 7239.

[21] W. Ji, G.-Q. Yue, F.-S. Ke, S. Wu, H.-B. Zhao, L.-Y. Chen, S.-Y. Wang, Y. Jia, *J. Korean Phys. Soc.* **2012**, *60*, 1253.

[22] K. J. Chen, A. D. Laurent, F. Boucher, F. Odobel, D. Jacquemin, *J. Mater. Chem. A* **2016**, *4*, 2217.

[23] L. Tsetseris, *J. Phys. Condens. Matter* **2016**, *28*, 295801.

[24] W. Setyawan, S. Curtarolo, *Comput. Mater. Sci.* **2010**, *49*, 299.

[25] W. Wu, Z. Jin, Z. Hua, Y. Fu, J. Qiu, *Electrochim. Acta* **2005**, *50*, 2343.

[26] Y. Ni, Z. Jin, Y. Fu, *J. Am. Ceram. Soc.* **2007**, *90*, 2966.

[27] X.-D. Gao, X.-M. Li, W.-D. Yu, J.-J. Qiu, X.-Y. Gan, *Thin Solid Films* **2008**, *517*, 554.

[28] M. Kim, S. Park, J. Jeong, D. Shin, J. Kim, S. H. Ryu, K. S. Kim, H. Lee, Y. Yi, *J. Phys. Chem. Lett.* **2016**, 2856.

[29] J. E. Medvedeva, in *Transparent Electronics: From Synthesis to Applications* (Eds.: A. Facchetti, T.J. Marks), John Wiley & Sons, Chichester, UK, **2010**, pp. 1–29.

[30] P. P. Boix, G. Larramona, A. Jacob, B. Delatouche, I. Mora-Sero, J. Bisquert, *J. Phys. Chem. C* **2012**, *116*, 1579.

[31] B. O'Regan, D. T. Schwartz, *Chem. Mater.* **1995**, *7*, 1349.

[32] K. Tennakone, G. R. R. A. Kumara, I. R. M. Kottegoda, V. P. S. Perera, G. M. L. P. Aponsu, *J. Phys. D. Appl. Phys.* **1998**, *31*, 2326.

[33] J. W. Jung, C. C. Chueh, A. K. Y. Jen, *Adv. Energy Mater.* **2015**, *5*, 1.

[34] E. Ruiz, S. Alvarez, P. Alemany, R. a Evarestov, *Phys. Rev. B* **1997**, *56*, 7189.

[35] A. Önsten, M. Månsson, T. Claesson, T. Muro, T. Matsushita, T. Nakamura, T.

Kinoshita, U. O. Karlsson, O. Tjernberg, *Phys. Rev. B* **2007**, *76*, 115127.

[36] V. P. S. Perera, M. K. I. Senevirathna, P. K. D. D. P. Pitigala, K. Tennakone, *Sol. Energy Mater. Sol. Cells* **2005**, *86*, 443.

[37] C. A. N. Fernando, I. Kumarawadu, K. Takahashi, A. Kitagawa, M. Suzuki, *Sol. Energy Mater. Sol. Cells* **1999**, *58*, 337.

[38] J. A. Dobado, R. Uggla, M. R. Sundberg, J. Molina, *J. Chem. Soc. Dalt. Trans.* **1999**, 489.

[39] S. B. Zhang, S.-H. Wei, A. Zunger, *Phys. Rev. B* **2001**, *63*, 75205.

[40] H. Raebiger, S. Lany, A. Zunger, *Phys. Rev. B* **2007**, *76*, 45209.

[41] a. Togo, F. Oba, I. Tanaka, K. Tatsumi, *Phys. Rev. B* **2006**, *74*, 195128.

[42] L. Tsetseris, *Phys. Chem. Chem. Phys.* **2016**, *18*, 7837.

[43] X. Liu, J. George, S. Maintz, R. Dronskowski, *Angew. Chemie Int. Ed.* **2015**, *54*, 1954.

[44] L. Tsetseris, *Phys. Chem. Chem. Phys.* **2016**, *18*, 14662.

[45] C. Liu, W. Wu, K. Liu, M. Li, G. Hu, H. Xu, *CrystEngComm* **2012**, *14*, 6750.

[46] T. Iwamoto, Y. Ogawa, L. Sun, M. S. White, E. D. Glowacki, M. C. Scharber, N. S. Sariciftci, K. Manseki, T. Sugiura, T. Yoshida, *J. Phys. Chem. C* **2014**, *118*, 16581.

[47] I. Mora-Seró, S. Giménez, F. Fabregat-Santiago, E. Azaceta, R. Tena-Zaera, J. Bisquert, *Phys. Chem. Chem. Phys.* **2011**, *13*, 7162.

[48] P. Pattanasattayavong, A. D. Mottram, F. Yan, T. D. Anthopoulos, *Adv. Funct. Mater.* **2015**, *25*, 6802.

[49] M. Grünewald, P. Thomas, D. Würtz, *Phys. status solidi* **1980**, *100*, K139.

[50] D. Monroe, *Phys. Rev. Lett.* **1985**, *54*, 146.

[51] M. H. Cohen, E. N. Economou, C. M. Soukoulis, *J. Non. Cryst. Solids* **1984**, *66*, 285.

[52] J. Orenstein, M. Kastner, *Phys. Rev. Lett.* **1981**, *46*, 1421.

[53] D. Aldakov, C. Chappaz-Gillot, R. Salazar, V. Delaye, K. A. Welsby, V. Ivanova, P. R. Dunstan, *J. Phys. Chem. C* **2014**, *118*, 16095.

[54] M. Shur, M. Hack, *J. Appl. Phys.* **1984**, *55*, 3831.

[55] P. G. Le Comber, W. E. Spear, *Phys. Rev. Lett.* **1970**, *25*, 509.

[56] P. G. Le Comber, A. Madan, W. E. Spear, *J. Non. Cryst. Solids* **1972**, *11*, 219.

[57] F. R. Shapiro, D. Adler, *J. Non. Cryst. Solids* **1985**, *74*, 189.

[58] S. D. Baranovskii, T. Faber, F. Hensel, P. Thomas, *J. Phys. Condens. Matter* **1997**, *9*, 2699.

[59] A. Manceau, D. L. Gallup, *Environ. Sci. Technol.* **1997**, *31*, 968.

[60] L. K. H. K. Alwis, M. R. Mucalo, B. Ingham, P. Kappen, *J. Electrochem. Soc.* **2015**, *162*, H434.

[61] X. Zhang, X. Zhao, Y. Jing, D. Wu, Z. Zhou, *Phys. Chem. Chem. Phys.* **2015**, *17*, 31872.

[62] B. L. Evans, A. D. Yoffe, P. Gray, *Chem. Rev.* **1959**, *59*, 515.

[63] J. A. Christians, R. C. M. Fung, P. V. Kamat, *J. Am. Chem. Soc.* **2014**, *136*, 758.

[64] Y. Peng, N. Yaacobi-Gross, A. K. Perumal, H. A. Faber, G. Vourlias, P. A. Patsalas, D. D. C. Bradley, Z. He, T. D. Anthopoulos, *Appl. Phys. Lett.* **2015**, *106*, 243302.

[65] W. Sun, S. Ye, H. Rao, Y. Li, Z. Liu, L. Xiao, Z. Chen, Z. Bian, C. Huang, *Nanoscale* **2016**, *8*, 15954.

[66] C. Choi, J. Y. Gorecki, Z. Fang, M. Allen, S. Li, L.-Y. Lin, C.-C. Cheng, C. Chang, *J. Mater. Chem. C* **2016**, *4*, 10309.

[67] M. Grundmann, F.-L. Schein, M. Lorenz, T. Böntgen, J. Lenzner, H. von Wenckstern, *Phys. status solidi* **2013**, *210*, 1671.

Figure 1. (a) Crystal structure of hexagonal β-CuSCN. Atoms are color-coded as dark brown for Cu, yellow for S, grey for C, and blue for N. (b) Electronic band structure of hexagonal β-CuSCN calculated by DFT with HSE hybrid functional. Reproduced from Ref.[22] with permission from The Royal Society of Chemistry. Copyright 2016, The Royal Society of Chemistry. (c) Brillouin zone of a hexagonal lattice showing the high-symmetry path typically used in the electronic band structure calculations. Reprinted from Computational Materials Science, Vol. 49, W. Setyawan and S. Curtarolo, High-throughput electronic band structure calculations: Challenges and tools, pp. 299-312,[24] Copyright 2010, with permission from Elsevier.

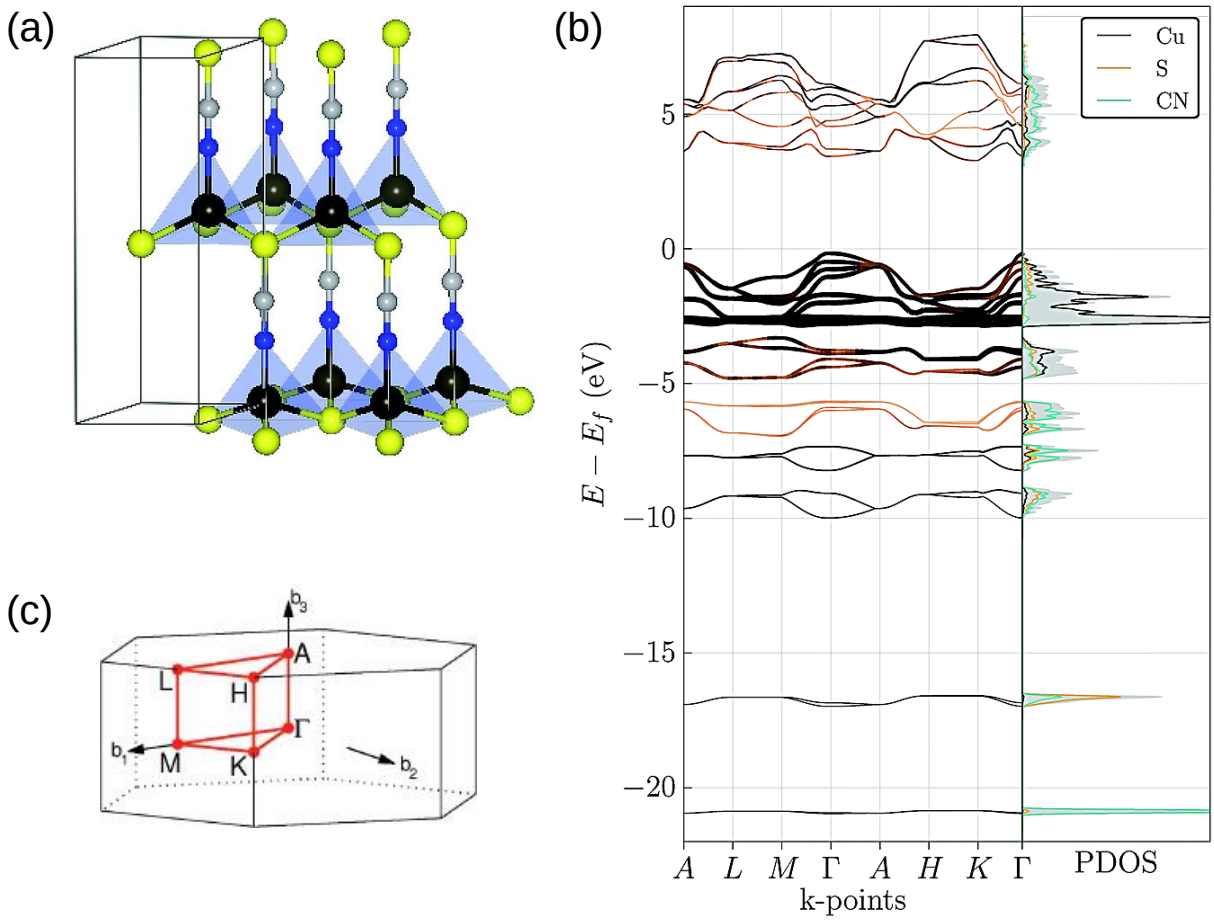

Figure 2. (a) Calculated total and partial densities of states of hexagonal β-CuSCN showing the contributions from different states of the constituents of CuSCN. Reprinted with permission from J. Phys. Chem. C 2010, 114, 9111.[11] Copyright 2010 American Chemical Society. (b) Measured photoemission spectrum near the valence band edge of CuSCN. Features in the spectrum are labelled based on the calculated DOS shown in (a). From Chem. Commun. 2013, 49, 4154-4156[12] - Reproduced by permission of The Royal Society of Chemistry. Copyright 2013, The Royal Society of Chemistry.

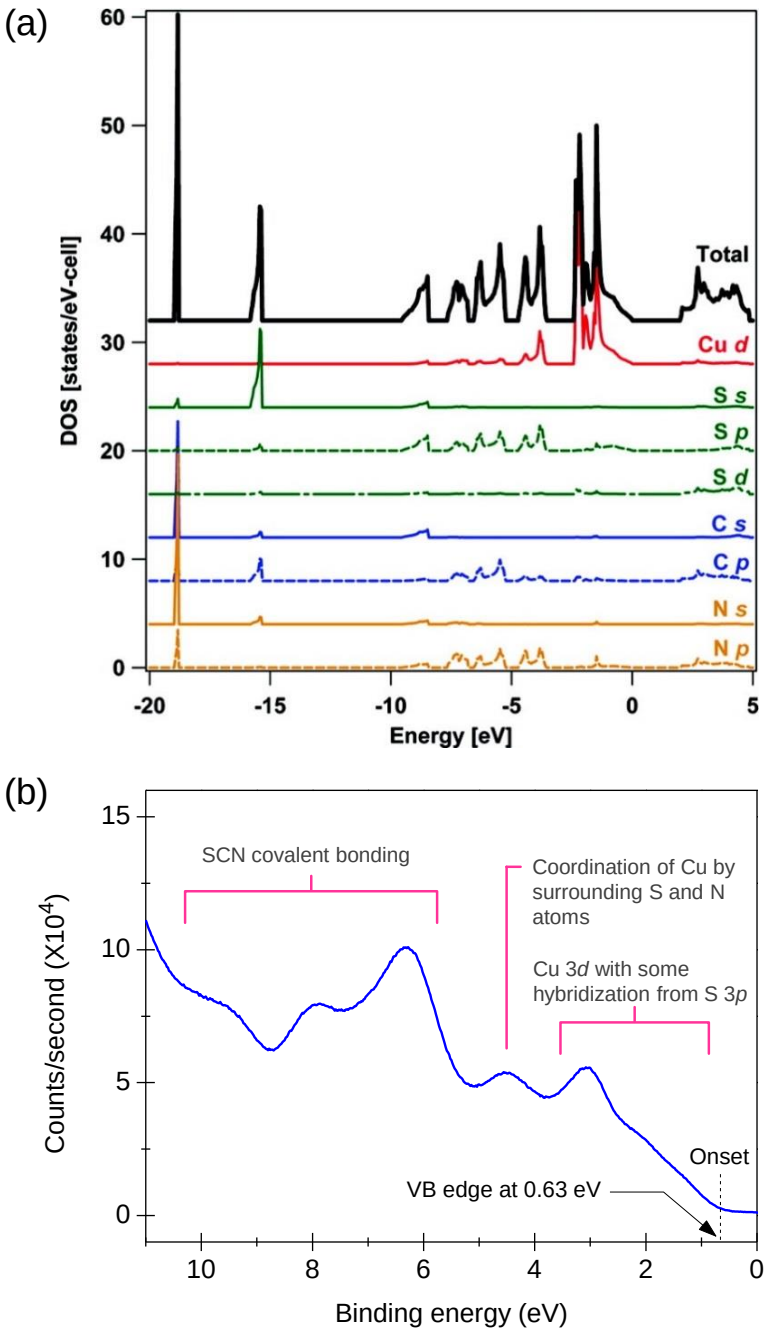

Figure 3. Single H impurity in hexagonal β-CuSCN forming (a) S–H bond and (b) C–H bond. (c) Two H impurities hydrogenating the cyanide portion. Atoms are color-coded as brown for Cu, yellow for S, grey for C, and blue for N. Copyright IOP Publishing. Reproduced with permission.[23] All rights reserved.

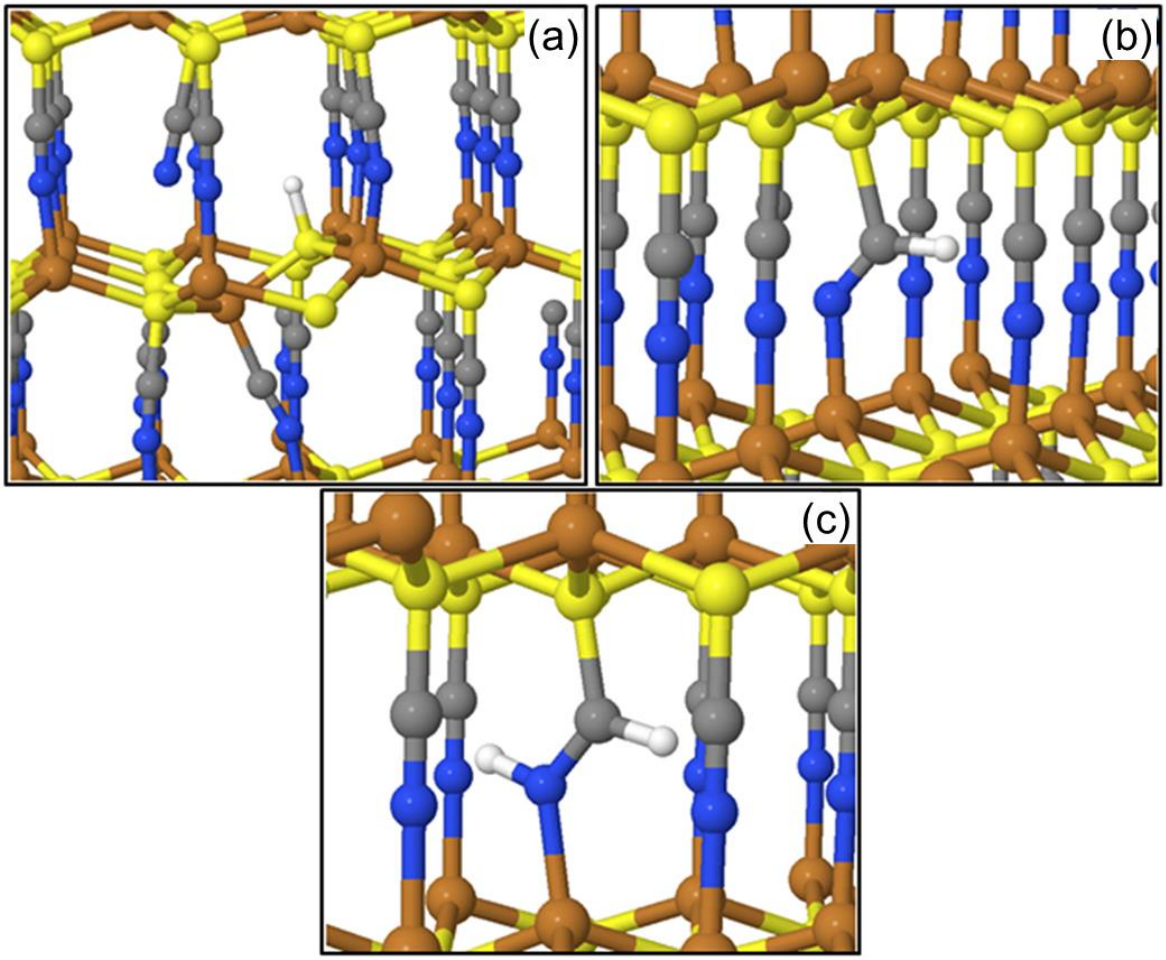

Figure 4. Two phases of bulk CuSCN which have been experimentally observed: (a) α and (b) β phases (the latter shown in the 2H polytype). Three newly predicted layered 2D-like phases: (c) γ, (d) δ, and (e) epsilon phases. Atoms are color-coded as brown for Cu, yellow for S, grey for C, and blue for N. Reproduced from Ref.[42] with permission from the PCCP Owner Societies. Copyright 2016, PCCP Owner Societies.

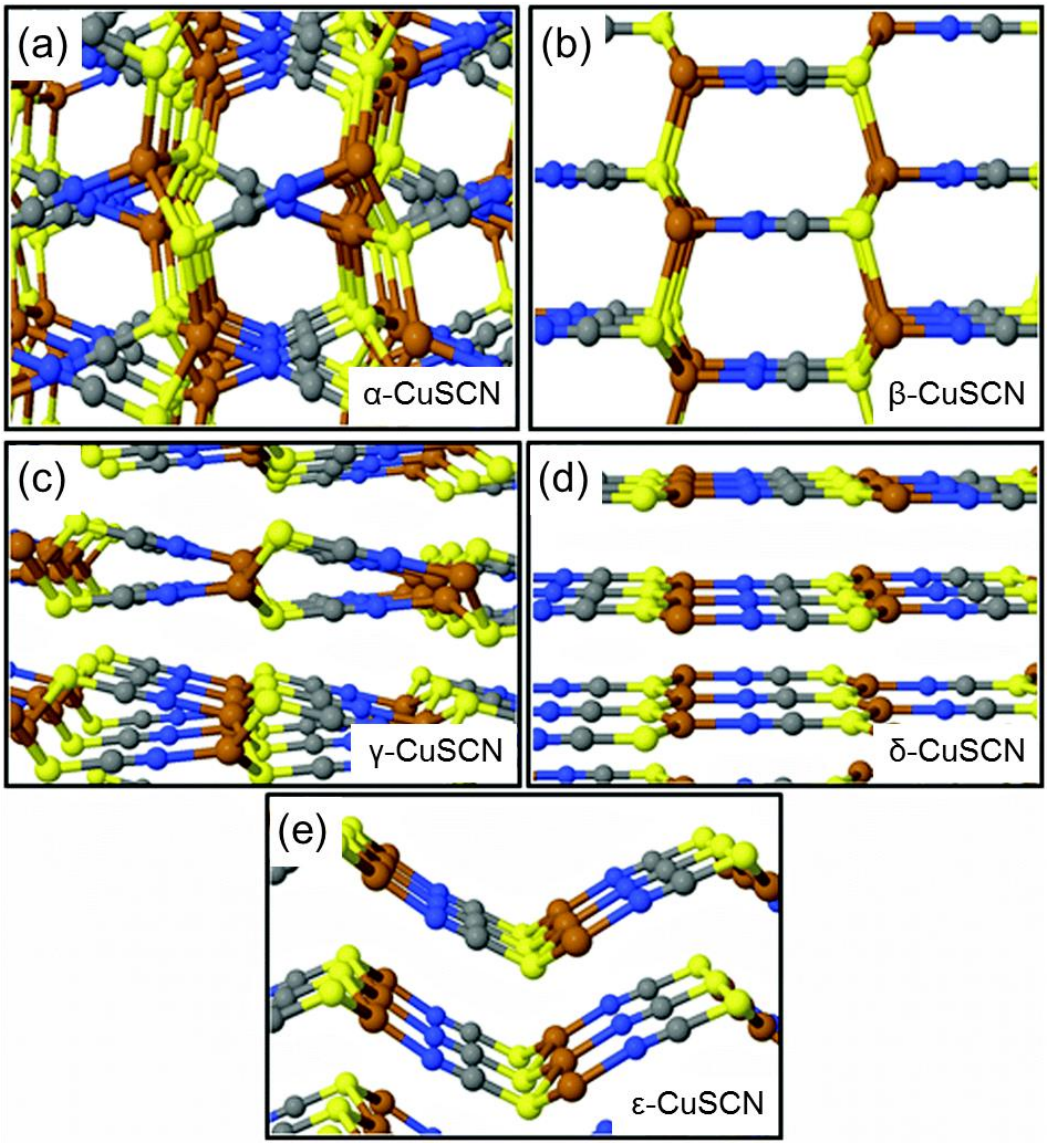

Figure 5. Slabs of hexagonal β-CuSCN displaying the non-polar (110) and (100) surfaces in (a) and (b), respectively, and the polar (101) and (001) surfaces in (c) and (d), respectively. The images are shown as side views with the surfaces orthogonal to the page and the plane normal pointing to the top of the page. Atoms are color-coded as dark brown for Cu, yellow for S, grey for C, and blue for N. Reproduced from Ref.[22] with permission from The Royal Society of Chemistry. Copyright 2016, The Royal Society of Chemistry.

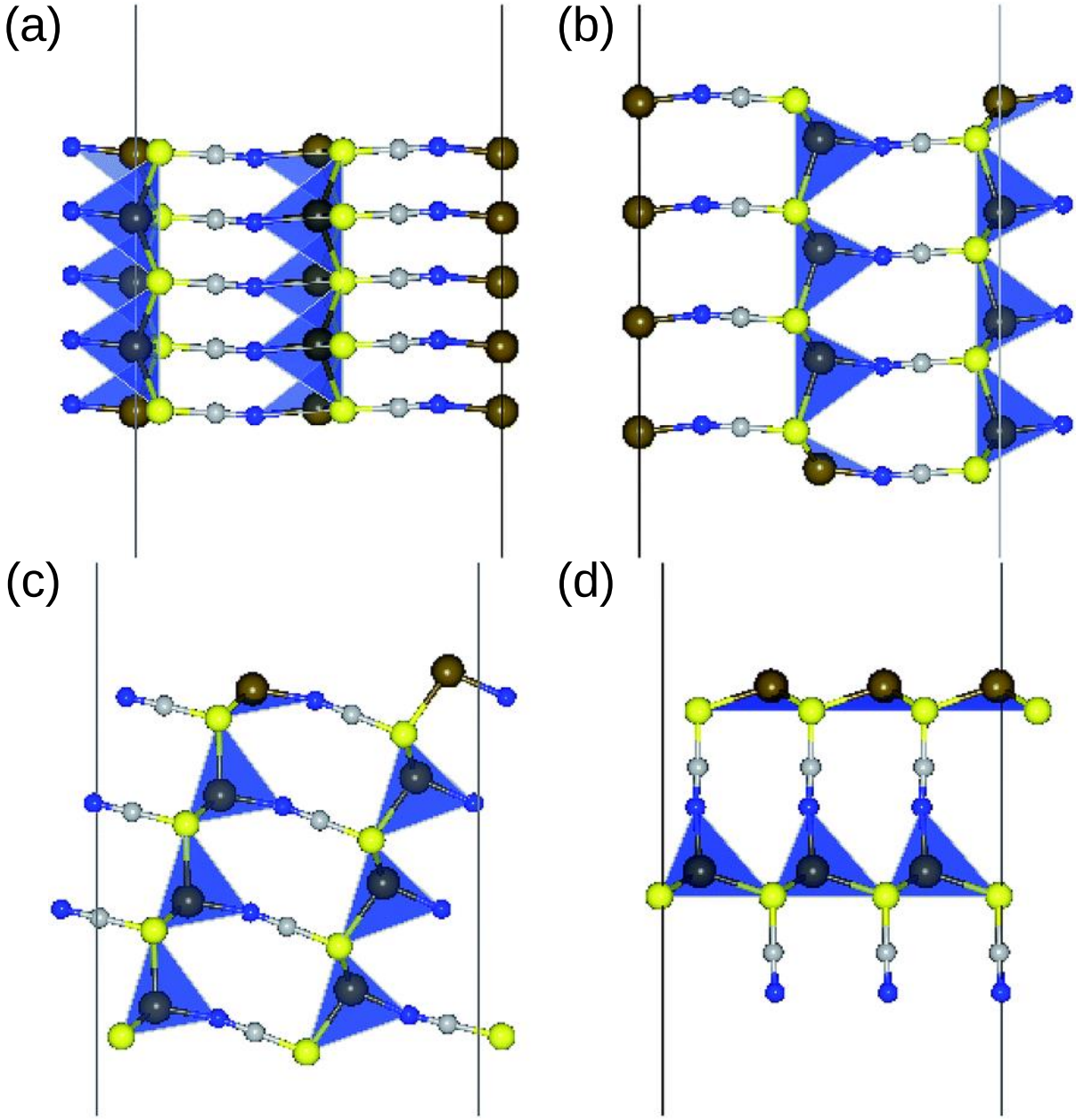

Figure 6. (a) Density of states of the tail localized states in the mobility gap of polycrystalline solution-processed CuSCN calculated from the transfer characteristics of CuSCN-based field-effect transistors. Reproduced with permission.[48] Copyright 2015, Wiley. (b) Photoemission spectrum near the valence band edge of CuSCN obtained using the He II UV source and (inset) the close-up showing the band-tail states extending from the valence band edge toward the Fermi level. Reprinted with permission from J. Phys. Chem. Lett. 2016, 2856.[28] Copyright 2016 American Chemical Society.

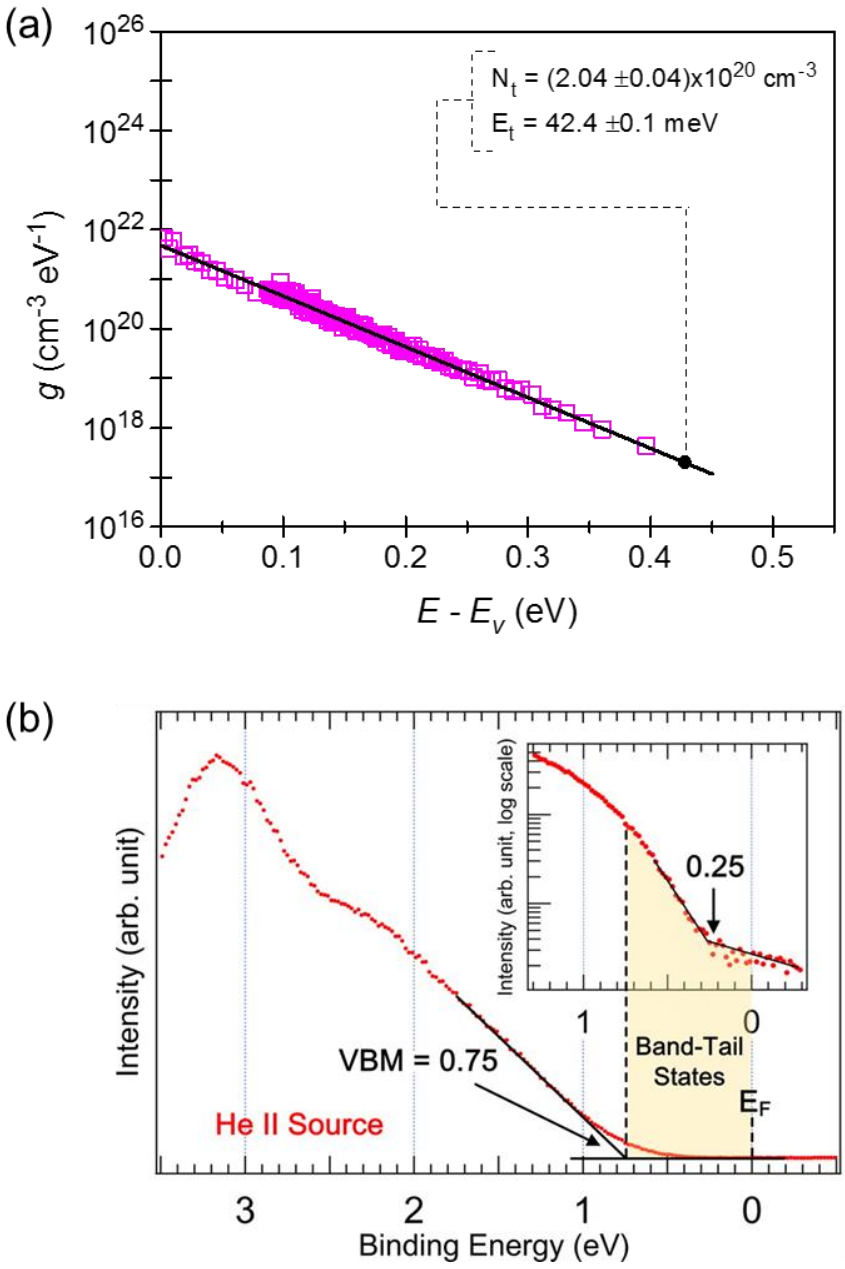

Pichaya Pattanasattayavong obtained his BEng in Nano-Engineering (First Class Honors, 2009) from Chulalongkorn University, Thailand. Awarded with a scholarship from Anandamahidol Foundation under the Royal Patronage of His Majesty the King of Thailand, he went on to receive his MSc (2010) and PhD (2014) in Physics from Imperial College London, UK. In 2015, he joined the School of Molecular Science and Engineering, Vidyasirimedhi Institute of Science and Technology (VISTEC), Thailand, as a lecturer. His current research interests include novel solution-processable materials for opto/electronic applications as well as semiconductor physics and charge transport physics of novel materials and devices.

Vinich Promarak received his D.Phil. degree in Chemistry from University of Oxford, UK, in 2002 and is currently a full Professor of Chemistry at School of Molecular Science and Engineering, Vidyasirimedhi Institute of Science and Technology (VISTEC), Thailand. His research interests involve around "high-tech" organic materials that can be used in applications such as organic light-emitting diodes, perovskite/dye-sensitized solar cells, bulk heterojunction solar cells, sensors, optical switches, organic field-effect transistors.

Thomas D. Anthopoulos received his D.Phil. degree in Physical Electronics from Staffordshire University, UK. He then spent two years at the University of St. Andrews (UK) where he worked on organic light-emitting diodes. In 2003 he joined Philips Research

Laboratories (The Netherlands) to work on organic integrated circuits. In 2005 he was awarded an EPSRC Advanced Fellowship and in 2007 a RCUK Fellowship both hosted in the Department of Physics, Imperial College London, where he is currently a Professor of Experimental Physics. His research interests are diverse and involve the development and application of novel nano-patterning paradigms, the physics of carbon-based, metal oxides and hybrid organic-inorganic semiconductors & devices and their applications.

Adv. Electron. Mater. **2017**, 1600378, DOI: 10.1002/aelm.201600378

Table of Contents Entry

The electronic and charge transport properties of the wide band gap, hole-transporting semiconductor copper(I) thiocyanate (CuSCN) are summarized and discussed herein. Emphasis is placed on the electronic band structure and density of states in CuSCN, defects and impurities, predicted novel two-dimensional layered structures, band tail states and hole transport properties in solution-processed CuSCN layers.

Keyword: Copper(I) thiocyanate (CuSCN); wide band gap semiconductor; hole transport, electronic band structure, defects, density functional theory (DFT)

P. Pattanasattayavong*, V. Promarak, Thomas D. Anthopoulos

Electronic Properties of Copper(I) Thiocyanate (CuSCN)

ToC Figure